



Share Your Innovations through JACS Directory

Journal of Nanoscience and Technology

Visit Journal at <http://www.jacsdirectory.com/jnst>

Strain Induced Modifications of Valence Band Features in Fe₃O₄ Epitaxial Heterostructures

Inderpal Singh^{1,*}, Sunil K. Arora¹, R.J. Choudhary²¹Centre for Nanoscience and Nanotechnology, Block-II, South Campus, Panjab University, Sector-25, Chandigarh – 160 014, Punjab, India.²UGC DAE Consortium for Scientific Research, Indore – 452 001, Madhya Pradesh, India.

ARTICLE DETAILS

Article history:

Received 03 October 2018

Accepted 22 October 2018

Available online 11 November 2018

Keywords:

Epitaxy

Valence Band

Energy Density Curves

ABSTRACT

We report systematic investigations of lattice mismatch strain and the strain relaxation induced modifications on the valence band electronic structure of the epitaxial Fe₃O₄/Si (100) and Fe₃O₄/MgO (100) heterostructures. The Fe₃O₄ films on Si (100) and MgO (100) substrates were investigated through the angle-integrated photoemission spectroscopy (AIPES) at room temperature in the energy range 45–65 eV. Depending on the strain state of the films, the Raman modes and the Verwey transition temperature show deviations from the corresponding bulk values. The valence band feature at 2.7 eV (3.5 eV) shifts towards (away) the Fermi level with an increase (decrease) in strain resulting in decrease (increase) of density of states (DOS) of the minority spin Fe(A) 3d-e_g band (majority spin Fe(B) 3d-t_{2g} band). The effect is more pronounced in the case of films on MgO (100) substrate in comparison to the films on Si (100) substrate.

1. Introduction

The interest in half-metallic materials has grown over the decades owing to their widespread application potential in spintronics (where the spin degrees of freedom are used in design of spin FET's, spin memory devices and quantum computing components) [1, 2]. Magnetite (Fe₃O₄) is one of the important material due to its interesting physical properties, such as, half-metallicity, high Curie temperature (850 K) and the Verwey transition (metal to insulator transition) at 125 K [3–5].

The half-metallic properties of the materials does depend on the density of states at the surface and at the fermi level (E_F), which could be measured using the highly sophisticated photoemission techniques utilizing the synchrotron flux. In the case of Fe₃O₄, the photoemission studies of the valence band electronic structure had been conducted in angle integrated and angle resolved modes on bulk, single crystal and thin films. Different substrates such as MgO, Pt, W, Fe/Mo have been used for the growth of epitaxial Fe₃O₄ thin films using different deposition techniques for the valence band features in Fe₃O₄ [6–8]. Strain is an important parameter in the thin film epitaxial growth that allows one to manipulate the electronic and magnetic properties of these films. There are theoretical reports that strain influence the valence band structure in the materials. Jeng et al. studied Fe₃O₄ thin film using the linear muffin-tin orbital method using density functional theory (DFT) and observed that the majority states showed conducting behaviour above a critical value of the applied in-plane strain in these films (-1.3% and 2.1 %) [9]. To the best of our knowledge hitherto, there are no systematic experimental investigation reported that correlate the effect of strain with the valence band structure in Fe₃O₄.

In this article, we report the modifications in the valence band features observed in differently strained Fe₃O₄ epitaxial layers through the use of angle integrated photoemission spectroscopy (AIPES) conducted at resonance energy of 58 eV. For these investigations, we considered two cases (i) strain originating due to the lattice mismatch between the film and the substrate (The lattice mismatch of Fe₃O₄ with Si (100) and MgO (100) is 15.1% and 0.34 % respectively) (ii) strain relaxation with the increase in the thickness (30 and 80 nm thickness) of the films.

2. Experimental Methods

The investigated Fe₃O₄ films were deposited by the pulsed laser deposition (PLD) technique (KrF excimer Laser source, λ = 248 nm, pulse width 20 ns) from α-Fe₂O₃ target (purity 99.999%) on single crystalline Si (100) and MgO (100) substrates. The substrates were cleaned differently prior to film deposition using the standard procedure described elsewhere [10]. The deposition was performed using the optimized parameters with vacuum better than 10⁻⁶ Torr [11]. The films thickness was determined to be 30 nm and 80 nm as determined using the X-ray reflectivity (XRR) measurements (Bruker D8 Diffractometer). The structural characterization of the films was performed using single crystal X-ray diffraction (XRD) rocking curves using Cu-K_α radiation (Rigaku, Japan). Magnetite phase was confirmed using the Raman spectroscopy (Jobin Yvon Horiba LABRAM-HR visible). The resistivity-temperature (R-T) measurements were performed using the physical property measurement system (PPMS) (in-lab designed).

The X-ray photoelectron spectroscopy (XPS) and valence band spectroscopy (VBS) studies have been conducted at AIPES beamline (BL-02) on the Indus-1 synchrotron radiation source at RRCAT, Indore (India). The core level XPS was performed on these films using the Mg-K_α source at room temperature (RT). The valence band studies of the epitaxial Fe₃O₄ films were investigated by AIPES at RT in the energy range 45–65 eV which covers the Fe 3p to 3d excitation threshold. These spectra were measured using an Omicron (EA-125) energy analyzer with resolution better than 0.6 eV for XPS and 0.03 eV for VBS studies. Au foil was used as a reference for the Fermi level (E_F).

3. Results and Discussion

Prior to discussing the valence band photoemission spectroscopy results, we would like to mention that the author's group in their previous work reported in detail the structural, magnetic, spin-transport behaviour and the local electronic structure of these hetero-epitaxial systems [10–14]. In our previous studies we demonstrated atomically flat interfaces of Fe₃O₄ with MgO substrates and studied their strain relaxation behaviour in detail [10]. Magnetic properties of the films can be altered through the growth conditions and the substrate cleaning procedures [12–14]. The local electronic structure of the films was found to be dependent on the strain in the films, which alters the Fe-O interatomic distances and further affects the site symmetry resulting in different binding energies of the Fe²⁺ and Fe³⁺ cations present at different interstices within the film [11].

*Corresponding Author: inder0691@gmail.com (Inderpal Singh)

3.1 Structural Characterization

3.1.1 X-Ray Diffraction Measurements

X-ray diffraction studies on all the samples confirmed that the films are stoichiometric and oriented in $\langle 111 \rangle$ and $\langle 100 \rangle$ directions on Si (100) and MgO (100) respectively. The films on Si (100) possessed lattice constant comparable to the bulk (0.839 nm) whereas the films on the MgO (100) showed fully strained behavior with an out-of-plane lattice constant deviating from the bulk (0.837 nm). The films of 30 nm thickness are fully strained whereas the 80 nm films were partially relaxed (20% strain relaxed).

3.1.2 Raman Measurements

Fig. 1 shows the Raman spectra of all the samples measured with the He-Ne laser (wavelength 633 nm) at 300 K with a laser power of 9 mW. As shown in Fig. 1, the Raman spectra exhibits characteristic A_{1g} , $T_{2g}(2)$ and $T_{2g}(3)$ Raman peaks at 670 cm^{-1} , 540 cm^{-1} and 310 cm^{-1} , confirm the magnetite (Fe_3O_4) phase in the films [15]. The $T_{2g}(2)$ peak in the Fe_3O_4 films on Si (100) cannot be analyzed due to its overlap with the high intense peak of the ω_{TO} mode of the Si(100) substrate. Detailed peak fitted parameters of the Raman peaks are summarized in the Table 1.

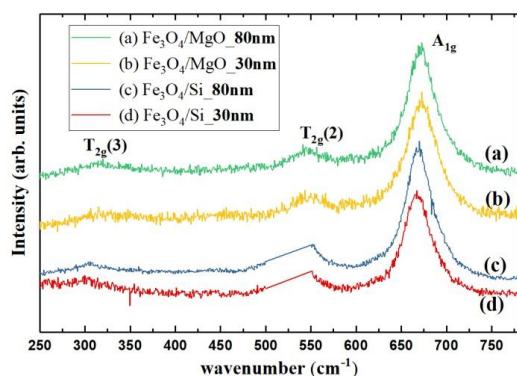


Fig. 1 Normalized Raman spectra of the Fe_3O_4 films of thickness (a) 80 nm (b) 30 nm on MgO (100) substrate and of thickness (c) 80 nm and (d) 30 nm Si (100) substrate. The $T_{2g}(2)$ peak in the Fe_3O_4 films on Si (100) has been removed due to the overlap of very high intense peak of the ω_{TO} mode of the Si(100) substrate

The Raman mode positions observed for the thin films shows a clear deviation from the corresponding value for the bulk Fe_3O_4 and an increased FWHM (due to strain present in the films). Higher is the strain present in the films greater is the deviation observed in the films. The A_{1g} modes are shifted to higher side for the films on MgO (100) with values 671.83 cm^{-1} and 672.09 cm^{-1} corresponding to 80 nm and 30 nm films. Whereas they are shifted to lower side for the films on Si (100) with values 669.29 cm^{-1} and 668.10 cm^{-1} corresponding to 80 nm and 30 nm films. We notice that the $T_{2g}(3)$ mode is affected the most showing a large shift to higher wavenumber i.e. at 317.85 cm^{-1} and 324.38 cm^{-1} for films on MgO (100) and at 305.10 cm^{-1} and 301.42 cm^{-1} for films on Si (100).

Table 1 Summary of the Raman peak positions and their FWHM for the A_{1g} , $T_{2g}(2)$ and $T_{2g}(3)$ Raman modes in Fe_3O_4 films of different thickness on MgO (100) and Si (100) substrates

Sample	A_{1g} mode		$T_{2g}(2)$ mode		$T_{2g}(3)$ mode	
	Position (cm^{-1})	FWHM (cm^{-1})	Position (cm^{-1})	FWHM (cm^{-1})	Position (cm^{-1})	FWHM (cm^{-1})
$\text{Fe}_3\text{O}_4/\text{MgO}_{80 \text{ nm}}$	671.83	40.04	544.37	43.47	317.85	63.34
$\text{Fe}_3\text{O}_4/\text{MgO}_{30 \text{ nm}}$	672.09	38.79	543.99	39.90	324.38	57.56
$\text{Fe}_3\text{O}_4/\text{Si}_{80 \text{ nm}}$	669.29	38.01	-	-	305.10	48.01
$\text{Fe}_3\text{O}_4/\text{Si}_{30 \text{ nm}}$	668.10	39.74	-	-	301.42	46.24

3.2 Resistivity Temperature Measurements

The temperature dependence of resistivity for all the samples is shown in Fig. 2. All the samples exhibit characteristic Verwey transition confirming the stoichiometric growth of Fe_3O_4 films. The Verwey transition is observed at 115 K and 107 K for films of 80 nm and 30 nm thickness on Si (100) whereas its values are 106 K and 100 K for the films on MgO (100) substrate. It is well known that the presence of the Verwey transition in Fe_3O_4 is a clear indication of the high quality stoichiometric films. Our results are in agreement with the other reports that the Verwey transition temperature of Fe_3O_4 is affected by the strain present in the films [10, 12].

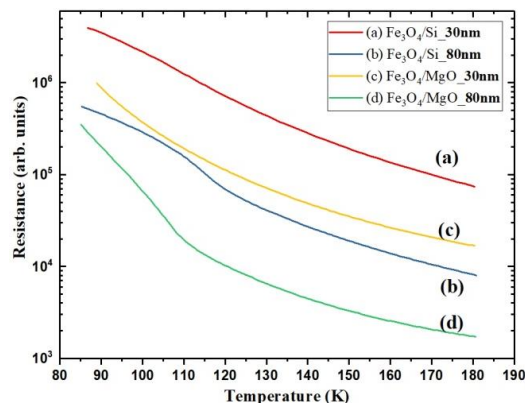


Fig. 2 Variation of the resistance with temperature in the vicinity of the Verwey transition for Fe_3O_4 films. The curves are shown for Fe_3O_4 films on Si (100) substrate for (a) 30 nm (b) 80 nm thickness and on MgO (100) substrate for (c) 30 nm (d) 80 nm thickness

3.3 Valence Electronic Structure Measurements

For the XPS and VBS measurements, the samples were transferred ex-situ to the analysis chamber. Prior to measurements, the samples were subjected to low energy Ar^+ ion sputter cleaning in the preparation chamber. Low energy (500 eV) of Ar^+ ions was selected to ensure that the cleaning procedure does not influence the surface and the composition of the films. Then, the samples were transferred to the analysis chamber with a base pressure better than 10^{-9} Torr. XPS studies on the as-grown samples at RT confirmed the Fe_3O_4 phase and stoichiometry. The $\text{Fe}^{3+}/\text{Fe}^{2+}$ ratio was found to be close to 2 [2/0.996 (2.114/1)] for Fe_3O_4 films on MgO (100) (Si(100)) substrates respectively. The detailed analysis and characterization of the core level XPS results has been reported in our previous publication [11].

Prior to performing the VBS measurements, the beam was scanned on the sample to get the maximum intensity across the multichannel analyzer (EA 125). The pass energy across the analyzer was set at 20 eV. The resolution throughout the measurements was better than 30 meV. The valence band spectra of the Fe_3O_4 were probed in the energy range 45-65 eV which covers the $3p$ to $3d$ excitation threshold. The energy density curves (EDC) showed resonance enhancement at 58 eV which is attributed to the final-state interference between the direct photoemission from the $3d$ levels ($3p^6 3d^n \rightarrow 3p^6 3d^{n+1} + e^-$) and the indirect Auger electron emission (Coster-Kronig transition) ($3p^6 3d^n \rightarrow [3p^5 3d^{n+1}]^* \rightarrow 3p^6 3d^{n-1} + e^-$). In order to measure the effect of strain on the as-grown films, the valence band EDC's for all samples were recorded at incident energy of 58 eV and incidence angle of 45° .

The obtained spectra were corrected for charging effects by taking into account the Fermi edge of Au foil and then normalized the intensity with respect to the beam current (Fig. 3). The background subtraction was done using the Shirley background correction procedure. The observed VBS spectra on Si (100) and MgO (100) are in agreement with the previously reported spectra for the $\langle 111 \rangle$ and $\langle 100 \rangle$ reported films respectively [16, 17]. Peak fitting for the normalized EDC's was done to determine the contribution of various known valence band features as illustrated in Fig. 4 for Fe_3O_4 (111) on Si (100). The features observed at 0.9 eV, 2.7 eV, 3.5 eV, 5.6 eV, 6.7 eV, 8.0 eV, 10.0 eV and 11.4 eV are in line with the previous report by Cai et al. of Fe_3O_4 films on Pt (111) substrate [7].

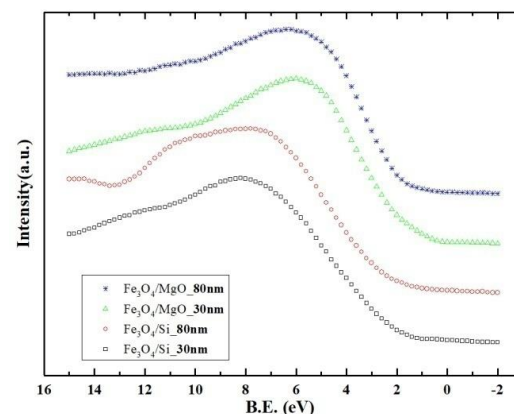


Fig. 3 Normalized valence band Energy density curves measured at RT with 58 eV incident energy

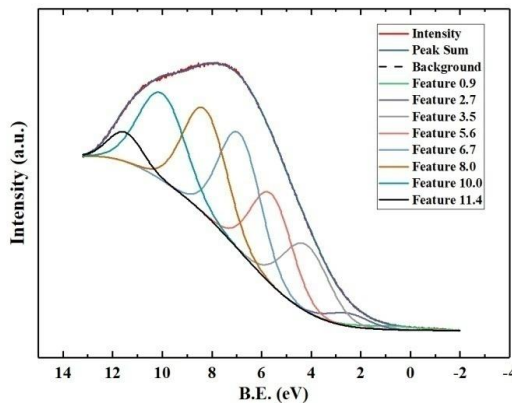


Fig. 4 Peak fitted spectra of $\text{Fe}_3\text{O}_4(111)/\text{Si}(100)$ taking Shirley background

The VB features observed for Fe_3O_4 films can be interpreted using the ionic model, according to which the O-2p derived states are present in the 3-8 eV binding energy range while the Fe 3d-derived states extends over 4eV below E_F [17]. Fig. 5 shows the EDC's for the films of thickness 30 nm and 80 nm on Si (100) and MgO (100) substrates. The feature at 0.9 eV is assigned to the final states of the Fe^{2+} ions, feature at 2.7 eV is due to the minority spin Fe(A) 3d- e_g band and feature at 3.5 eV is due to the majority spin Fe(B) 3d- t_{2g} band. The other features at higher binding energy are reflected as hybridization of Fe 3d-derived states and O-2p states. All the films show a finite density of states (DOS) at the E_F reflecting their metallic behaviour. The metallicity is greater for the films on the Si (100) substrate in comparison to the films on the MgO (100) substrate. Further the films of 30 nm (strained) show lower DOS at E_F than the films of 80 nm (relaxed). The strain present in the films reduces the metallic behaviour of the films.

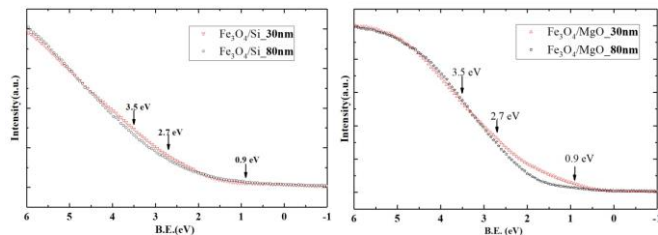


Fig. 5 Normalized Energy density curves of 30nm and 80nm thickness Fe_3O_4 films on (a) Si (b) MgO substrates

The observed deviations in the binding energy of the analyzed features for different samples are summarized in Table 2. For the Fe_3O_4 films on MgO (100) substrate, the feature at 0.9 eV remains unchanged in both the films. The feature at 2.7 eV is shifted towards E_F with a deviation of 0.84 eV on 30 nm film and 0.20 eV on 80 nm film on MgO (100). The feature at 3.5 eV is shifted towards E_F by 0.02 eV on 30 nm film and away from E_F by 0.43 eV on the 80 nm film. For the case of films on the Si (100) substrate, the feature at 0.9 eV and 2.7 eV on the film of 30 nm remains unchanged. For film of 80 nm thickness, the feature at 2.7 eV shift towards the E_F by 0.2 eV and the feature at 3.5 eV shift away by 0.71 eV. The features at higher binding energy are attributed to either hybridization with O-2p orbitals or the satellite features.

Table 2 Deviation of the fitted features on different samples. (↓ indicate the shift towards Fermi level (E_F) and ↑ indicate a shift toward increasing binding energy)

Valence band feature	$\text{Fe}_3\text{O}_4/\text{Si}$ (30 nm)	$\text{Fe}_3\text{O}_4/\text{Si}$ (80 nm)	$\text{Fe}_3\text{O}_4/\text{MgO}$ (30 nm)	$\text{Fe}_3\text{O}_4/\text{MgO}$ (80 nm)
0.9 eV	0	0	0	0
2.7 eV	0	0.20 ↓	0.84 ↓	0.2 ↓
3.5 eV	0.22 ↑	0.71 ↑	0.02 ↓	0.44 ↑

In order to understand the deviation of valence band features, we need to pay attention to the differences in strain state of the films. The feature at 0.9 eV reflects an increase in the DOS for films on MgO (100) with increasing strain as reflected in Fig. 5(b). The feature at 2.7 eV (3.5 eV) shifts towards (away) E_F with the increase (decrease) in strain as evident from the comparison of all the films. The shift towards E_F due to 2.7 eV decreases the DOS of the minority spin Fe(A) 3d- e_g band. The deviation of the 3.5 eV feature away from the E_F increases DOS for the majority spin Fe(B) 3d- t_{2g} band as inferred from Fig. 5.

Our observations are in line with the theoretical prediction that the strain affects the DOS for the majority and minority spin channels [9]. This can be understood from the fact that the lattice-mismatch strain affects the Fe-O interatomic distance which further affects the site symmetry and band structure. During the growth, the Fe_3O_4 epitaxial films suffer from various growth defects such as dislocations, anti-phase boundaries (APB's) etc. which in turn affects the strength of the crystal field and local symmetry affecting the band structure [18]. The impact of strain is more pronounced in the case of the heterostructures grown on MgO (100) substrate.

4. Conclusion

We used angle integrated photoemission spectroscopy to investigate the valence band features of Fe_3O_4 films grown on Si (100) and MgO (100) substrates. Impact of strain and growth induced defects are more pronounced in the case of Fe_3O_4 films grown on MgO (100) substrates. The observations verify our analysis that the strain relaxation with thickness of the films plays an important role in determining the valence band features.

Acknowledgement

We would like to express our gratitude to UGC-DAE consortium for scientific research, Indore, India and RRCAT, Indore, India for providing us infrastructure facility related to this work. Authors are also thankful to the DST for providing PURSE grant-II. One of the authors IS, thank UGC-DAE for the doctoral fellowship.

References

- [1] L. Zhang, W. Hou, G. Dong, Z. Zhou, S. Zhao, et al., Low voltage induced reversible magnetoelectric coupling in Fe_3O_4 thin films for voltage tunable spintronic devices, *Mater. Horiz.* 5 (2018) 991-999.
- [2] S.A. Wolf, D.D. Awschalom, R.A. Buhrman, J.M. Daughton, S. Von Molnár, et al., Spintronics: A spin-based electronics vision for the future, *Science* 294 (2001) 1488-1495.
- [3] I. Žutić, J. Fabian, S.D. Sarma, *Spintronics: Fundamentals and applications*, Rev. Mod. Phys. 76 (2004) 323-410.
- [4] M. Ziese, Extrinsic magnetotransport phenomena in ferromagnetic oxides, *Rep. Prog. Phys.* 65 (2002) 143-249.
- [5] E.J. Verwey, P.W. Haayman, Electronic conductivity and transition point of magnetite (Fe_3O_4), *Physica* 8 (1941) 979-987.
- [6] K. Shiratori, S. Suga, M. Taniguchi, K. Soda, S. Kimura, A. Yanase, Photoemission Study of Fe_3O_4 , *J. Phys. Soc. Jpn.* 55 (1986) 690-698.
- [7] Y.Q. Cai, M. Ritter, W. Weiss, A.M. Bradshaw, Valence-band structure of epitaxially grown Fe_3O_4 (111) films, *Phys. Rev. B* 58 (1998) 5043-5051.
- [8] W. Wang, J.M. Mariot, M.C. Richter, O. Heckmann, W. Ndiaye, et al., $\text{Fe } t_{2g}$ band dispersion and spin polarization in thin films of $\text{FeO}(001)/\text{MgO}(001)$: Half-metallicity of magnetite revisited, *Phys. Rev. B* 87 (2013) 085118-1-7.
- [9] H.T. Jeng, G.Y. Guo, First-principles investigations of the electronic structure and magnetocrystalline anisotropy in strained magnetite Fe_3O_4 , *Phys. Rev. B* 65 (2002) 094429-1-9.
- [10] S.K. Arora, R.G.S. Sofin, I.V. Shvets, Anomalous strain relaxation behavior of $\text{Fe}_3\text{O}_4/\text{MgO}(100)$ heteroepitaxial system grown using molecular beam epitaxy, *J. Appl. Phys.* 100 (2006) 073908-1-8.
- [11] I. Singh, S.K. Arora, M.G. Moinuddin, R.J. Choudhary, X-ray photoelectron spectroscopy studies of Fe_3O_4 films on Si and MgO substrates grown by pulsed laser deposition, *AIP Conf. Proc.* 1942 (2018) 080046-1-4.
- [12] R.G.S. Sofin, H.C. Wu, R. Ramos, S.K. Arora, I.V. Shvets, Influence of anisotropic strain relaxation on the magnetoresistance properties of epitaxial $\text{Fe}_3\text{O}_4(110)$ films, *J. Appl. Phys.* 118 (2015) 173903-1-6.
- [13] S.K. Arora, R.G.S. Sofin, I.V. Shvets, Magnetoresistance enhancement in epitaxial magnetite films grown on vicinal substrates, *Phys. Rev. B* 72 (2005) 134404-1-10.
- [14] S.K. Arora, H.C. Wu, R.J. Choudhary, I.V. Shvets, O.N. Mryasov, H. Yao, W.Y. Ching, Giant magnetic moment in epitaxial Fe_3O_4 thin films on MgO(100), *Phys. Rev. B* 77 (2008) 134443-1-5.
- [15] Shailja Tiwari, D.M. Phase, R.J. Choudhary, Probing antiphase boundaries in Fe_3O_4 thin films using micro-Raman spectroscopy, *Appl. Phys. Lett.* 93 (2008) 234108-1-4.
- [16] Y.S. Dedkov, M. Fonin, D.V. Vyalikh, J.O. Hauch, S.L. Molodtsov, U. Rüdiger, G. Güntherodt, Electronic structure of the $\text{Fe}_3\text{O}_4(111)$ surface, *Phys. Rev. B* 70 (2004) 073405-1-4.
- [17] R.J. Lad, V.E. Henrich, Photoemission study of the valence-band electronic structure in Fe_xO , Fe_3O_4 , and $\alpha\text{-Fe}_2\text{O}_3$ single crystals, *Phys. Rev. B* 39 (1989) 13478-13485.
- [18] Z. Huang, W. Liu, J. Yue, Q. Zhou, W. Zhang, Y. Lu, et al., Enhancing the spin-orbit coupling in Fe_3O_4 epitaxial thin films by interface engineering, *ACS Appl. Mater. Interf.* 8 (2016) 27353-27358.